Front. Struct. Civ. Eng. 2015, 9(4): 383–396
DOI 10.1007/s11709-015-0320-z

RESEARCH ARTICLE

Computational model generation and RVE design of self-healing concrete

Md. Shahriar QUAYUM[a], Xiaoying ZHUANG[a,b,*], Timon RABCZUK[a]

[a] *Institute of Structural Mechanics, Bauhaus-Universität Weimar, Weimar 99425, Germany*

[b] *Department of Geotechnical Engineering, College of Civil Engineering, Tongji University, Shanghai 200092, China*

[*] *Corresponding author. E-mail: xiaoyingzhuang@tongji.edu.cn*

ABSTRACT Computational homogenization is a versatile tool that can extract effective properties of heterogeneous or composite material through averaging technique. Self-healing concrete (SHC) is a heterogeneous material which has different constituents as cement matrix, sand and healing agent carrying capsules. Computational homogenization tool is applied in this paper to evaluate the effective properties of self-healing concrete. With this technique, macro and micro scales are bridged together which forms the basis for multi-scale modeling. Representative volume element (RVE) is a small (microscopic) cell which contains all the microphases of the microstructure. This paper presents a technique for RVE design of SHC and shows the influence of volume fractions of different constituents, RVE size and mesh uniformity on the homogenization results.

KEYWORDS homogenization, self-healing concrete (SHC), representative volume element, multiscale modelling

1 Introduction

Concrete is a vastly used building material. It is very prone to crack formation as it has lower tensile strength. The detection and repairing of cracks are very difficult and expensive. That is why self-healing is very important and appropriate for concrete. The hydration of cement clinker is a long on-going process. So, in the lifetime of concrete there is some unhydrated cement, which when comes in contact with water can hydrate itself [1].

Dry [2] first proposed to introduce self-healing properties in concrete. The pioneering research on autonomic self healing of concrete was carried out by White et al. [3]. They investigated self healing by encapsulating chemicals in polymeric materials. Several experiments were carried out to investigate the method of encapsulation, sensing and actuation of releasing encapsulated chemicals by Dry [2,4], Li et al. [5], Lee et al. [6] as mentioned in Ref. [7]. Li et al. [5] demonstrated the actuation of chemical release by crack formation in concrete, which results in breaking the embedded brittle hollow glass fibers containing the polymer [7].

Article history: Received Apr 15, 2015; Accepted Sept 30, 2015

To do a large scale simulation it is often required to have a homogeneous property of a microscopically composite material. This require homogenization technique which can extract effective elastic properties from the fine scale model to the coarse scale model. With this aim, various theories have been developed from the rule of mixtures to effective medium models of Eshelby, Hashin, Mori and Tanaka. There are other closed-form analytical or semi-analytical homogenization techniques like Voigt-Reuss-Hill bounds, Hashin-Shtrikman variational principle, self-consistent method etc. [8]. The computational homogenization technique was initiated by Suquet [9], Guedes and Kikuchi [10], Terada and Kikuchi [11], Ghosh et al. [12–13].

In recent years, significant progress has been made in two-scale homogenization of multi-phase solids. A nested two-scale solution can be achieved through parallel computation which can reduce huge computational cost as mentioned by Kouznetsove et al. [14]. In two-scale homogenization, two important attributes need special attention as mentioned by Yuan and Fish [15]. One is multiple overall strain loading, periodic boundary conditions etc. Another is scale bridging mechanism, which essentially includes proper data transfer and manipulation between the scales.

In this paper, the homogenization tool is applied for extracting the effective properties of self-healing concrete and the numerical results are compared with the analytical results.

2 Multiscale methods for SHC

Focus on one particular scale is a traditional approach for modeling, where the smaller scales are modeled with constitutive relation and the larger scales are modeled assuming the system as homogeneous. But this traditional approach has some disadvantage as inherent material flaws of small scales are neglected in large scales, which may lead to some sort of failure. This is omitted in multiscale modeling approach. When empirical coarse-grained models are inadequate, the macroscale behavior still can reflect the system behavior with the help of microscale models [16].

In general, a coarse-grained model can describe a system adequately. There are some exceptions where some small regions of that coarse-grained model require detailed observations. These small regions may have defects, singularities or some critical events. This is the case where the model has different complexity in different regions. For this kind of problem, a coupling strategy needs to be adopted to couple the fine and coarse-grained model to have a comparable accurate result to that of only coarse-grained model.

Multiscale models can be categorised in two broad categories:

Hierarchical/sequential modeling: In this modeling method, the larger scale gets the information (e.g., elastic moduli) from finer scales. Then the larger scale mechanical response is taken using the information from finer scale. The response (e.g., deformation) is passed back again to the fine scale model. The computed stress strain from that fine scale model are averaged and sent back to coarse scale model [17]. This process involves multiple length scales from model hierarchy sequentially for computing mechanical response and hence this method is called hierarchical or sequential method.

Concurrent modeling: In this technique, the model couples different length scales concurrently i.e., parallely. Since, there are some problems involving critical regions where inelastic deformation occurs and other regions with elastic deformation; it is clearly computationally cheap to use large scale for elastic deformation regions and fine scale for inelastic regions. This also ensures relatively high accuracy without spending high computational effort. The inelastic region needs to be well defined for applying fine scale. The widely used example of concurrent multiscale modeling is crack propagation problem.

Semi-concurrent/ hybrid modeling: A drawback of the concurrent multiscale method is that the computational cost and memory requirement increase significantly with increasing size of the zone of interest (i.e., due to large crack growth or diffuse damage [18]). On the contrary, semi-concurrent models preserve microstructural information by linking each integration point of the macro-scopic domain to a unique unit-cell boundary value problem (BVP) of the microscopic domain. The BVP is defined on a RVE which is responsible for determining the macroscopic response of the integration point. This method passes information from fine scale to coarse scale and vice versa. Despite increased computational cost of semi-concurrent method over hierarchical method, the uncoupled nature of the BVP allows parallelization of the microstructural solution [18]. A classical semi-concurrent method is FE^2 method, where the strain response (e.g., deformation gradient) is passed from the coarse-scale to the fine-scale and the stress response is sent back from fine to coarse-scale [19]. The stress tensor is computed based on first order homogenization theory.

2.1 Hierarchical modeling of SHC

The self healing concrete is a composite structure that has different microphases namely cement matrix, sand particles or fine aggregates and healing agent containing capsules. The hierarchical multiscale modeling approach can utilize the microscale domains of geometry and individual mechanical properties of each microphase to obtain combined or effective macroscale mechanical responses. This modeling technique can couple micro with macro scale responses.

2.1.1 Microscale modeling

The microstructural configuration includes the geometry and mechanical properties of individual microphases like concrete, sand and capsules. In this model the cell containing all the microphases is termed as RVE. This RVE size selection is of great importance. The RVE size should be large enough to represent the detailed morphology of the microstructure. On the other hand, it should be sufficiently small to neglect the gradient of macroscopic mechanical response. The reason for the later is that, the physical and mechanical properties of each phase can be treated as independent of the material position [20].

2.1.2 Macroscale modeling

The existence of individual microphases of microscale model are considered to be eloped in macroscale model both geometrically and mechanically, whereas in macroscale model the new single homogeneous geometry exhibits effective or homogenized mechanical properties from all the microphases. This macroscale model should be large enough compared to the microscale model. Periodicity is an important assumption for multiscale modeling as it implies the repetition of unit cells in macro domain. The

global periodicity refers the uniform distribution of microstructure morphology. A more realistic periodicity assumption is local periodicity which assumes nonuniform distribution of microstructure morphology at the macroscopic level.

2.2 Analytical models

Mori-Tanaka model and self-consistent models are used as analytical tools for comparing homogenization results of 2D single phase composite. Following are the analytical models that are used for multi-phase composite.

2.2.1 Multi-phase composite: Two-step homogenization (MT-Voigt)

The homogenization of multi-phase composites needs two steps. The first step generally calculates the stiffness tensor for individual type of inclusions. Then the second step calculates the overall stiffness tensor for the composites from the inclusions stiffness tensors. The schematic view of two- step homogenization is shown in Fig. 1.

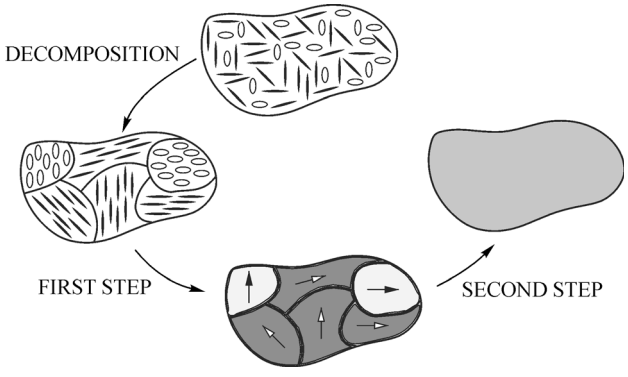

Fig. 1 The schematic representation of two-step homogenization [21]

The steps are discussed below:

1) 1st step: Homogenization of each type of grain individually

This step can be done by analytical Mori-Tanaka model for each type of grain α in the composite.

$$C_\alpha^{MT} = C_m + v_f(C_f C_m)A^{Eshelby}[(v_m I + \ v_f A^{Eshelby}]^{-1}, \quad (1)$$

where, C_α^{MT} refers to the Mori-Tanaka stiffness of inclusion type α; C_m, C_f refer to matrix stiffness and inclusion stiffness of the same inclusion type respectively; v_m, v_f refer to volume fraction of matrix and inclusion respectively; I is the identity tensor and $A^{Eshelby}$ is the dilute strain concentration tensor.

2) 2nd step: Homogenization of all types of grains

This step actually can be done by one of several models like Voigt or Reuss model. Here Voigt model is used. The stiffness tensor of whole composite according the this model is

$$C^{Voigt} = \ <C_\alpha>= \frac{\sum C_\alpha V_\alpha}{V}, \quad (2)$$

where V and V_α are the volume of composite and volume of each type of inclusion.

Special case: The capsules are modeled with a core inside and a thin shell surrounding core. So it is difficult to model the shell and core individually. Three methods have been implemented to apply two-step homogenization in this case.

2.2.2 MT-Voigt (effective interface) model

Effective interface model is used here to find the effective stiffness tensor of the particle with interface [22]. The model is schematically represented in Fig. 2. This is a modified Mori-Tanaka model for composites having particles with interface. The effective interface has a finite size and same spherical shape as the effective particle. Subscript "m" is used for matrix, "f" is used for fiber or particle without interface, "p" is used for particle core having surrounding interface and "i" is used for interface or shell.

The steps for this model are discussed below:

At first, the dilute strain concentration tensor A^p and A^{pi} for the particle core and combined core + shell of interface particle are calculated with the following formula-

$$A^p = I - \ S[S + (C_p - \ C_m)^{-1}C_m]^{-1}, \quad (3)$$

$$A^{pi} = I - S\left\{\frac{v_p}{v_i \ + v_p}[S + (C_p - C_m)^{-1}C_m \ ]^{-1} + \frac{v_i}{v_i \ + v_p}[S \ + (C_i \ - \ C_m)^{-1}C_m \ ]^{-1}\right\}. \quad (4)$$

Then the stiffness tensor of matrix with the particle having interface is calculated from the following formula:

$$C^{eff.int.} = C^m + [(v_p + v_i \ )(C_i - C_m)A^{pi} + v_p(C_p - C_i)A^p \ ][v_m I + (v_p + v_i)A^{pi}]^{-1}, \quad (5)$$

where, S refers in both equations to the corresponding Eshelby tensor of particle core and shell material; v_p and v_i are volume fractions of core and shell respectively; C_m, C_p and C_i refer to the stiffness tensor of matrix, particle core and shell respectively.

The stiffness tensor of matrix with particle without interface i.e., sand in case of SHC, is also calculated from the usual Mori-Tanaka formula.

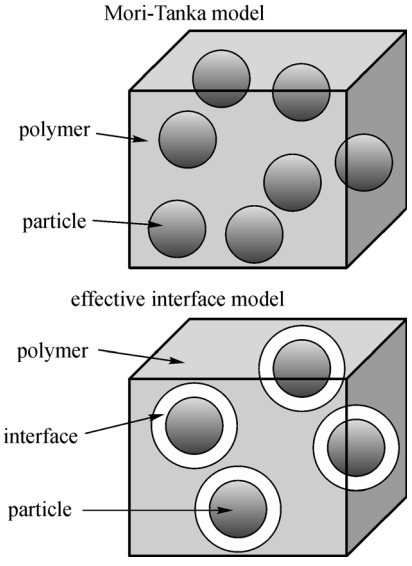

Fig. 2 Schematic illustration of Mori-Tanaka and effective interface micromechanics approaches [22]

2.2.3 MT-Voigt (method 1)

In this method, the composite is considered to be composed of 3 types of inclusion materials namely (sand, capsule core-MMA, capsule shell-Urea Formaldehyde). The core is surrounded by the shell material, which is different from sand particles which are surrounded by matrix material. So, the Eshelby tensor, S of core is calculated from the shell material's Poisson's ratio (shell material acting as surrounding matrix for the core), whereas Eshelby tensor of shell and sand is calculated from the matrix material's Poisson's ratio. Also for calculating strain concentration tensor, $A^{Eshelby}$ of core and Mori-Tanaka stiffness, C_p^{MT}; shell stiffness is taken as C_m .

$$C_p^{\mathrm{MT}} = C_m + v_p(C_p - C_i)A^{Eshelby}[v_i\mathrm{I} + v_pA^{Eshelby}]^{-1}. \quad (6)$$

2.2.4 MT-Voigt (method 2)

The capsule is comprised of shell and core. So the effective elastic properties of capsules are calculated using the following formula:

$$E_{cap} = \frac{E_{shell}V_{shell} + E_{core}V_{core}}{V_{shell} + V_{core}}, \quad (7)$$

where E refers to the elastic properties like Young's modulus, Poisson's ratio of corresponding subscripted materials and V refers to the volume of corresponding subscripted materials.

Then, the composite is considered to be comprised of two types of inclusions namely (sand, capsule). The elastic properties of capsules, calculated in the above mentioned method, were used to calculate the Mori-Tanaka stiffness in two-step method considering only two types of inclusions.

3 RVE design

The microstructure including both geometry and properties is characterized by representative volume element (RVE). The RVE should be small enough to allow computational time to be short and large enough to exclude non-existing properties (e.g., undesired anisotropy). There are different ways to define RVE mentioned by different authors. According to Drugan and Willis [23], an RVE should be a statistically representative sample of the microstructure, i.e., it should include virtually a sampling of all possible microstructral configuration as mentioned in Ref. [24]. This definition leads to a considerable large RVE for a non-uniform microstructure which is computationally inefficient. Therefore, this definition is rarely used in actual homogenization analyses. Another definition characterizes RVE to be the smallest possible microstructure that sufficiently represents the overall macroscopic properties of interest. This definition leads to a much smaller RVE sizes than the statistical definition given before. The RVE satisfying this definition does not always include an adequate distribution of microfields in RVE. The next definition is closer to the definition given by Hill [25]. From Hill's definition De Bellis [24] deduced that an RVE is well-defined if it reflects the microstructure and the response of the microstructure under uniform displacement boundary conditions and traction boundary conditions coincide. If a microstructural cell has less information about the microstructure, then the response will differ in uniform displacement boundary condition and traction boundary condition. The homogenization properties will not be effective properties, rather they will be "apparent" properties. The apparent properties by applying uniform displacement boundary condition usually overestimates the effective properties and the uniform traction boundary conditions usually underestimates the effective properties. Viewing the fact, several authors like Van der Sluis et al. [26], Terada et al. [27] have verified that the periodic boundary conditions provide better estimation of the overall effective properties for a given microstructure. The apparent properties with different uniform boundary condition on a microstructure becomes convergent with the increase in microstructure cell size as shown in Fig. 3. This has been investigated by Terada et al. [27], Huet [28,29], Ostoja-Starzewski [30,31], and Pecullan et al. [32]. This fact is also true for periodic boundary condition, while the convergence is reached with smaller cell size than that of uniform boundary conditions. So, in general it can be said that, estimation of the overall properties of a microstructure reaches to "convergence" with the increase of cell size.

3.1 Generation of RVE geometry

The geometry of RVE is to generate at first. At this point, the generation of a 2D RVE will be discussed. The following constituents are supposed to exist in the model- (a) cement matrix, (b) sand particles, (c) microcapsules containing the healing agent. The size of the 2D model considered for simulation ranges from 10 to 100 mm. Cement matrix part is considered as a homogeneous continuum in which the sand particles and the microcapsules are embedded. The geometry and distribution of sand and microcapsules are discussed below.

3.1.1 Sand particles

In Portland cement concrete (PCC), the concrete is comprised of cement (10%–15%), coarse and fine aggregates (60%–75%) and water (15%–20%) by volume. Fine aggregates makes up 20% to 35% of the total volume of the mix ("Foundry sand in portland cement concrete", http://www.afsinc.org/content.cfm?ItemNumber = 7116, July, 2014). The particle size distribution of sand particles for RVE size 100 mm is taken from a real sample of sieve analysis ("Sieve analysis test, the university of texas at arlington", http://www.uta.edu/ce/geotech/lab/Main/sieve/index.htm, July, 2014) and the sieve analysis result is shown in Table 1.

Approximate number of sand particles in the RVE can be obtained by a sample calculation similar to that of Table 2. In that table, the first and last size ranges are excluded from modeling consideration due to very large and very small particle diameters respectively. Also, for simplicity of calculation the weight percentage is considered as volume percentage (area percentage).

3.1.2 Microcapsules

The microcapsules are considered to be circular (in 2D) and spherical (in 3D). In this paper, the microcapsules are formed by containing liquid healing agent methyl

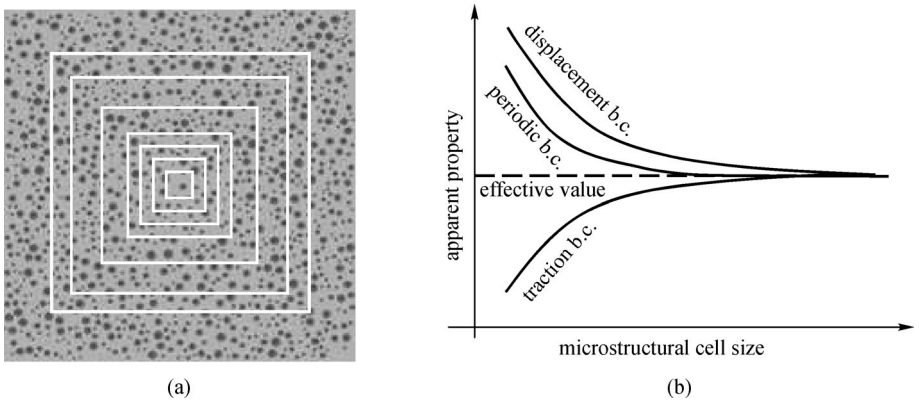

Fig. 3 (a) Microstructural cells of different sizes, (b) convergence of the apparent properties of effective values with increase of RVE size for different boundary conditions [33]

Table 1 A sample calculation of sieve analysis obtained from sieve analysis test, the university of texas at Arlington (http://www.uta.edu/ce/geotech/lab/Main/sieve/index.htm, July, 2014)

sieve No.	sieve opening/mm	mass of soil retained on each sieve, W_n/g	percentage of mass retained on each sieve, R_n	cumulative percent retained, ΣR_n	percent finer 100-ΣR_n
4	4.75	154	18.7	18.7	81.3
8	2.36	72	8.7	27.4	72.6
16	1.18	72	8.7	36.1	63.9
30	0.6	141	17.1	53.2	46.8
40	0.425	85	10.3	63.5	36.5
50	0.3	80	9.7	73.2	26.8
100	0.15	149	18.1	91.3	8.7
200	0.075	45	5.5	96.8	3.2
Pan	—	24	2.9	99.7	
		$\sum$ = 822 g = W_1			

mass of oven dry sample, W_t= 824 g
mass loss during sieve analysis, = (824 – 822)/824*100 = 0.2 = 2.0%

Table 2 Calculation of sand particles for a 100 mm×100 mm RVE

sieve No.	size range/mm	avg. dia./mm	weight distribu/gm	weight/%
4	4.75-2.361	3.56	0	
8	2.36-1.181	1.77	72	24.16
16	1.18-0.61	0.89	141	47.32
30	0.6-0.31	0.45	85	28.52
50	0.3-0.151	0.23	0	0.00

sieve No.	[a]sand area accord. to weight %/mm^2	(area÷particle)/mm^2	No. of particles reqd.	considered No. of particles
4	–	–	–	–
8	483.22	2.46	196.39	196
16	946.31	0.62	1521.12	1520
30	570.47	0.16	3586.89	3585
50	–	–	–	–

[a] Total sand area (considering 20% area of matrix which is 100 * 100 = 10000 mm^2) = 2000 mm^2

methacrylate. (MMA) within urea formaldehyde shell. The diameter of the capsules can vary according to the agitation rate in experiments [34]. For 2D RVE, the diameter is also restricted to 0.5–3.0 mm. The capsule shell thickness is considered as dia./27(from real microcapsule thickness/dia ratio as mentioned in Ref. [35]). It has been observed from the tests that, with a small amount of microcapsule (about 3%), flexural strength of concrete increases up to 3% and compressive strength up to 9% [36]. For RVE size 100 mm × 100 mm, the number of capsules generated are 100 which constitute, capsule to matrix ratio as 2.67%, so according to [36] this quantity will not decrease the flexural or compressive strength. So, the volumetric ratios obtained from sand and microcapsules with cement matrix are:

- Sand/matrix = 20.93%
- Capsule/matrix = 2.67%

3.1.3 Material properties

The material properties considered for different parts of RVE are summarized in Table 3.

As mentioned before, for the RVE, the healing agent is considered as MMA, while a small amount of PMMA is added to the MMA to increase the viscosity of fluid as mentioned in paper [35]. Though the healing agent is a liquid, for modeling simplicity it is considered as solid. The modulus of elasticity, E is taken from Matbase: Pmma properties (http://www.matbase.com/material-categories/natural-and-synthetic-polymers/commodity-polymers/material-properties-of-polymethyl-methacrylate-extruded-acrylic-html#properties, July, 2014), but as this is not a solid pure PMMA, the modulus is lower than the given value. Also, for being liquid, the Poisson's ratio should be less than but near to 0.5. So, 0.45 is considered as the Poisson's ratio for healing agent.

The mechanical properties of microcapsules were tested with urea formaldehyde (UF) shell and epoxy healing agent as capsule constituents in experiments [36–37]. The surface morphology of a capsule with UF wall along with its cross section is shown in Fig. 4. Since, actual mechanical tests have not been carried out in concrete structures [40], this is a scope for future works.

4 Homogenization results

The homogenization results are greatly affected by the

Table 3 Material properties considered for the RVE

material	Young's modulus, E/MPa	Poisson's ratio, v
cement matrix	14.848e3[a] (15e3 considered)	0.33
sand	10 – 28 (30 considered)	0.15 – 0.25 (0.2 considered)
capsule Shell[b]	3.60e3	0.3
capsule fluid[c]	1000	0.45

[a] E value was calculated from Ref. [38] with the following formula: $E_{hcp} = 29\ \text{GPa}*(1 - n_c)^3$, where, n_c = capillary porosity of hcp = 0.2 [39]
[b] the properties are obtained from Ref. [37]
[c] the properties are obtained from Matbase: Pmma properties (http://www.matbase.com/material-categories/natural-and-synthetic-polymers/commodity-polymers/material-properties-of-polymethyl-methacrylate-extruded-acrylic-html#properties, July, 2014)

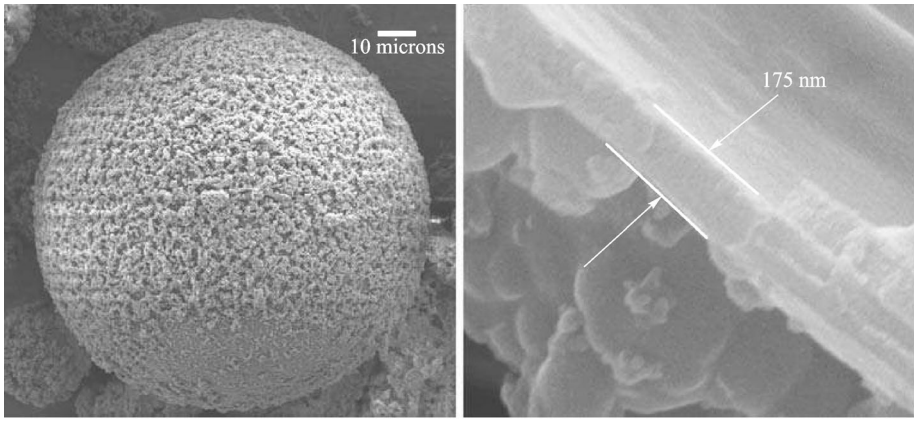

Fig. 4 (a)Surface morphology of a capsule with UF wall, (b) cross-section of the shell wall [37]

non-uniformity of mesh on boundaries, inclusion's volume fraction and RVE size. The non-uniformity of mesh is represented by seed difference of opposite boundaries. The log (error) against the seed difference plot of Fig. 5 shows that the Young's modulus, E11 (as the seed difference is only in 11 direction) and shear modulus, G has the similar trend of error over the seed difference, the trend of which is increasing with increasing seed difference. The error of Poisson's ratio and L^2 error norm of the elasticity tensor also shows the similar increasing trend with increasing seed difference.

4.1 Effect of variation of volume fraction of sands

The effect of volume fraction of sand particles on homogenized properties is shown in Fig. 6. The graph shows that the homogenization results are converging with lower volume fraction of inclusion which agrees with the assumption of analytical solution.

4.2 Effect of variation of RVE size with random distribution of sands and capsules

The sample size and different volume fractions of the constituents are shown in Table 4. The image of the samples are shown in Fig. 7.

In Fig. 8, the graphs show that the homogenization results are converging with the analytical solution with the increasing RVE size. The reason of this convergence with increasing RVE size is that the volume fraction of inclusions decrease with increasing RVE size which can be seen from Table 4.

4.3 3D homogenization results

The homogenization results of 3D RVE are shown for different RVE size with random distribution of sands and capsules in Fig. 10. The volume fraction of sands and capsules are given in Table 5 and the sample model images

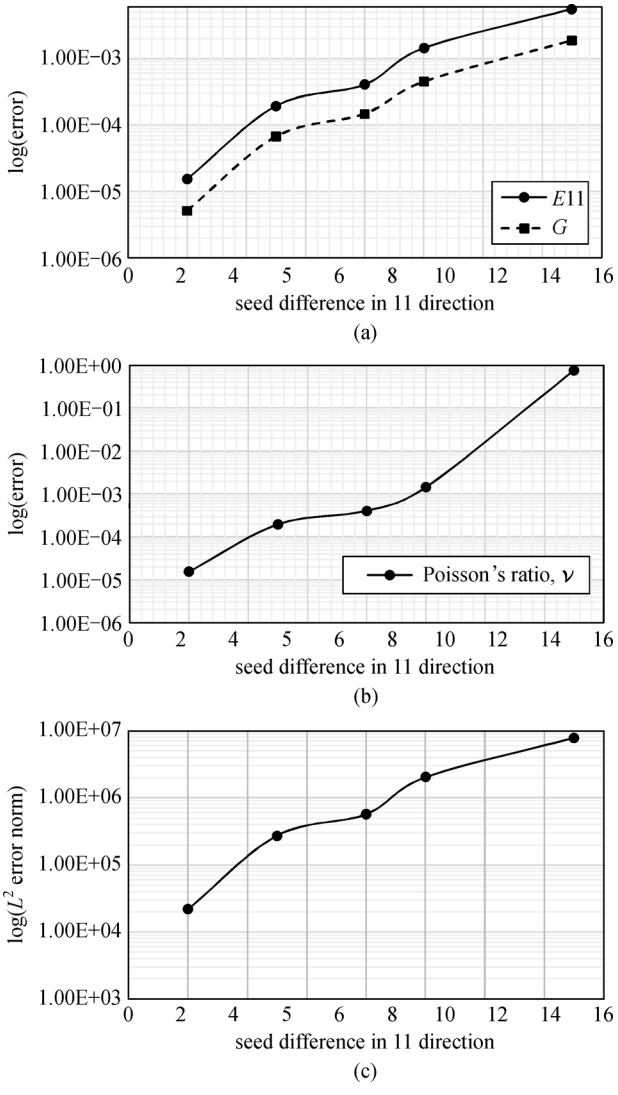

Fig. 5 Error plots of elastic properties against seed difference on opposite boundaries of 2D RVE in 11 direction

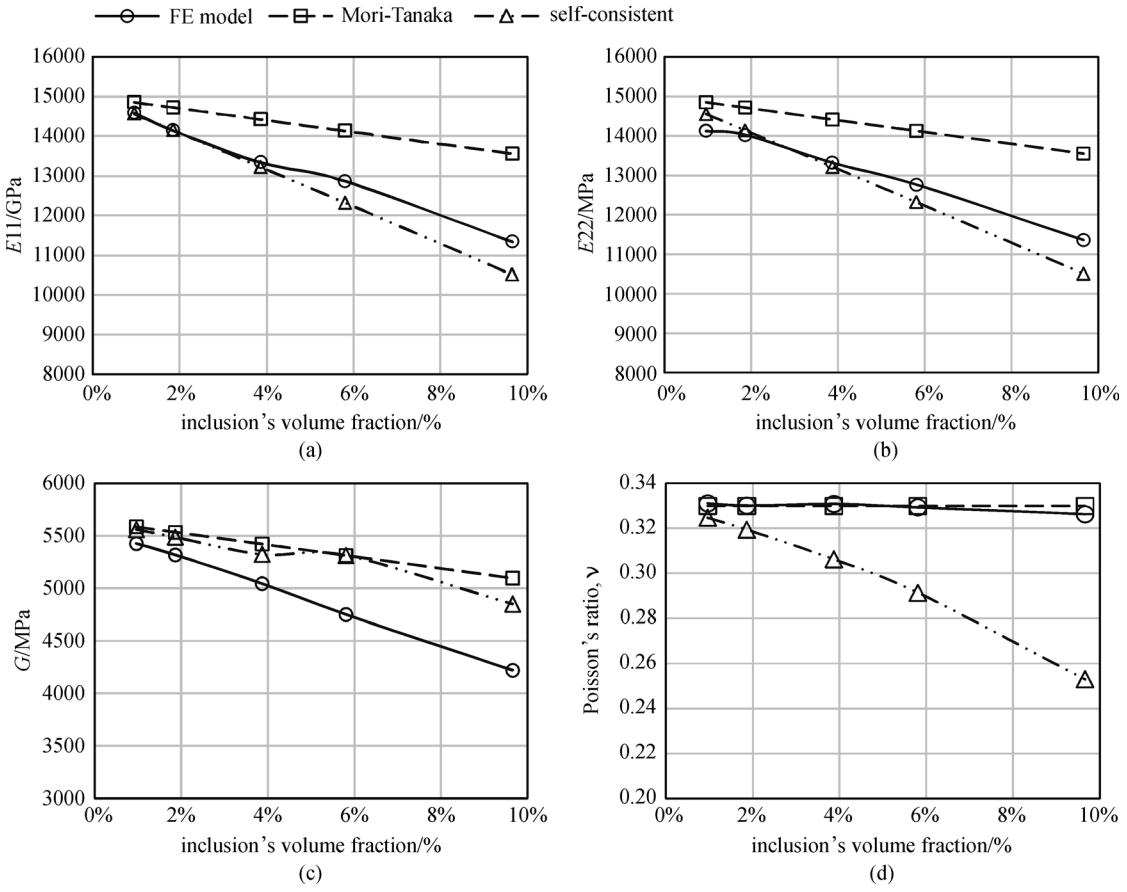

Fig. 6 Elastic properties against different volume fraction of sand in same RVE length

Table 4 RVE sizes and different constituents' volume fraction

model	RVE size/mm	matrix	sand	cap core	cap shell
FE1	100	78.73%	18.67%	2.23%	0.37%
FE2	50	78.17%	18.15%	3.16%	0.51%
FE3	40	77.27%	19.01%	3.19%	0.53%
FE4	30	76.23%	20.53%	2.79%	0.45%
FE5	20	75.20%	21.67%	2.72%	0.41%
FE6	10	73.39%	22.01%	4.00%	0.60%

Table 5 Volume fractions of different constituents of 3D RVEs

RVE size/mm	volume fraction/%			
	matrix	sand	cap shell	cap core
5	93.57	6.41	0.02	8.00E-06
8	89.89	6.22	0.73	3.16
10	88.03	10.24	0.34	1.39
15	83.02	13.38	0.74	2.86
20	83.01	12.74	0.84	3.41
25	86.8	9.86	0.67	2.67

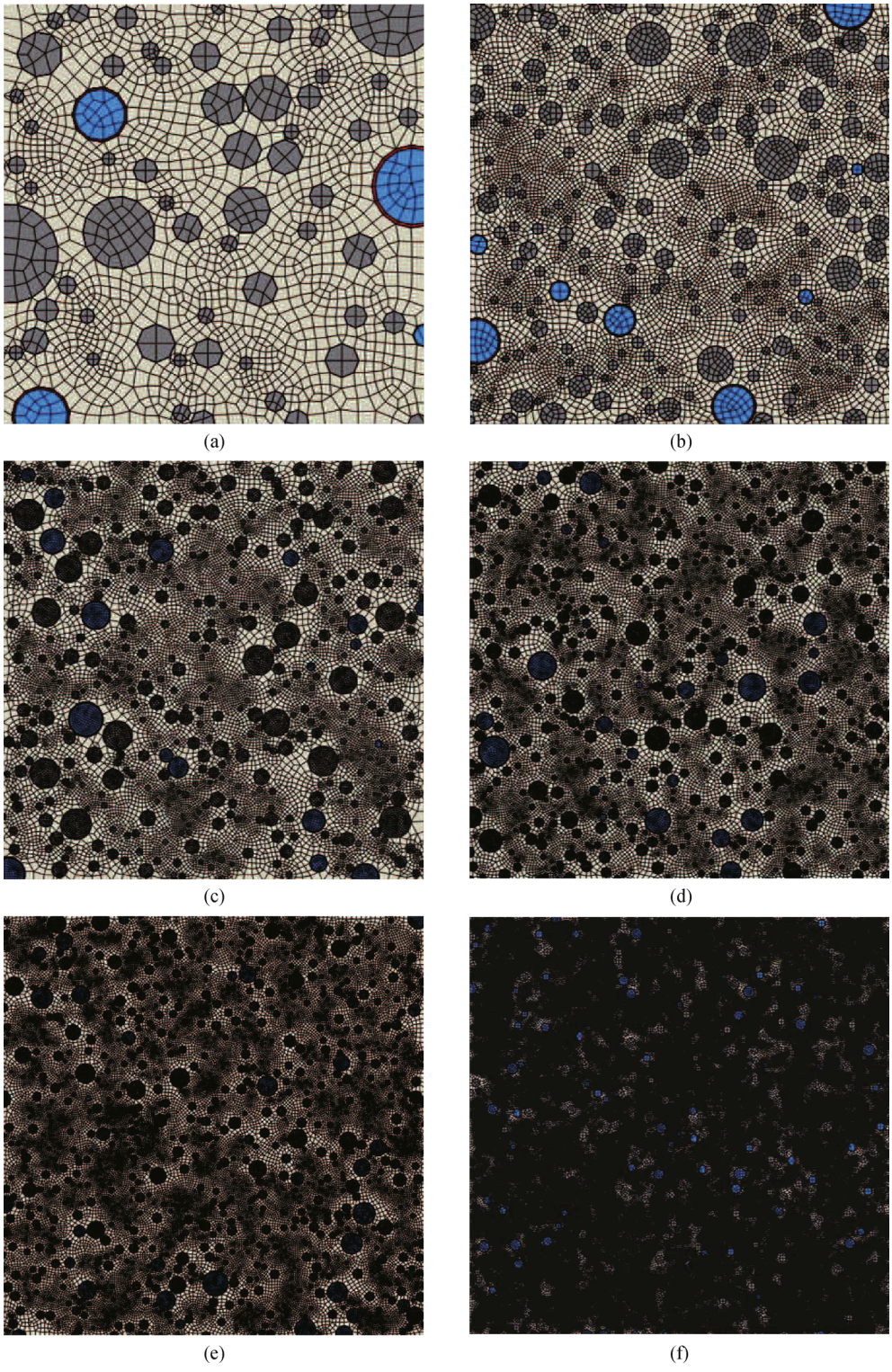

Fig. 7 Different RVE sizes with random sand and capsule distributions. (a) FE6:size 10 mm; (b) FE5:size 20 mm; (c) FE4:size 30 mm; (d) FE3:size 40 mm; (e) FE2:size 50 mm; (f) FE1:size 100 mm

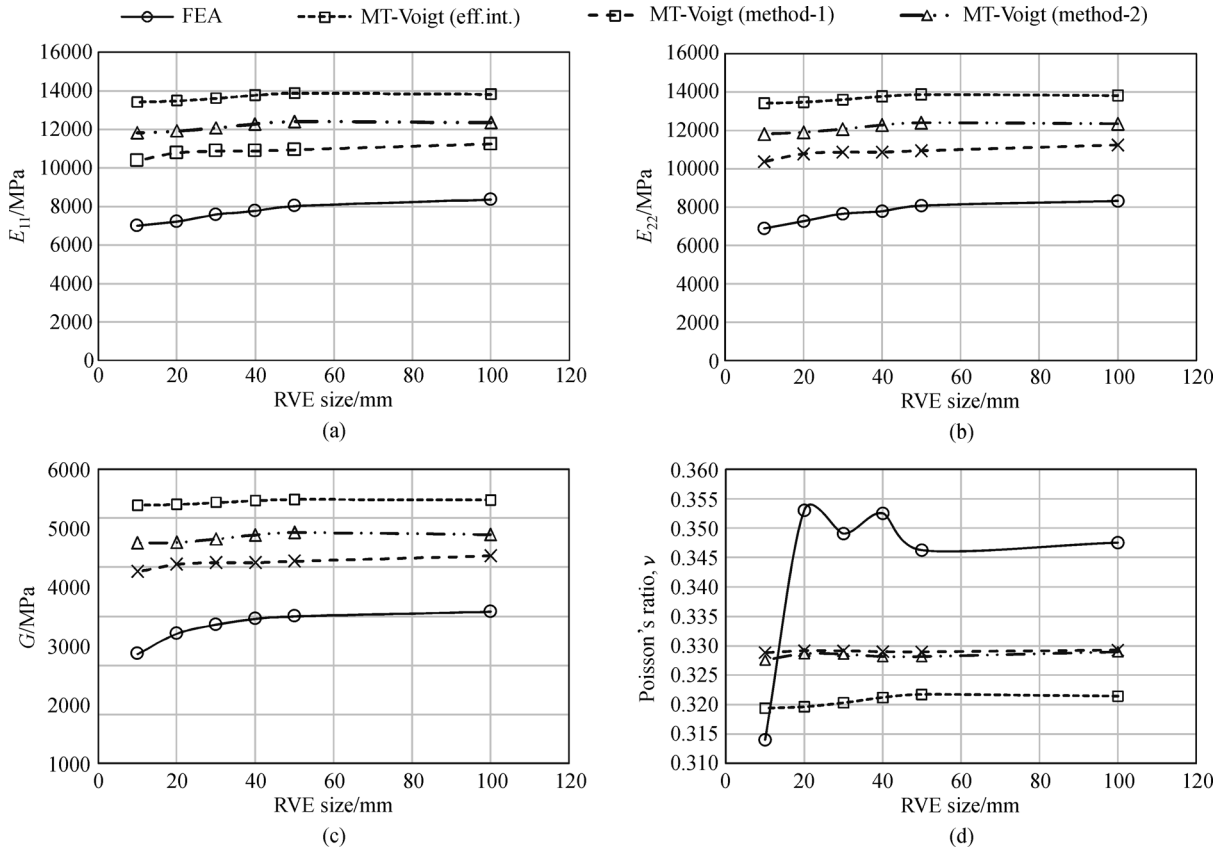

Fig. 8 Variation of elastic properties against different length of RVE with random distribution of capsules and sands; and comparison with analytical solution

are shown in Fig. 9. The error plots of Fig. 11 and L^2 error norm plot against the RVE size in Fig. 12 show that error reduces with decrease in RVE size. This agrees with the assumption of analytical solution which holds better results for lower volume fraction of inclusions, as the volume fraction is less in smaller RVE size in Table 5.

5 Discussion

Computational model generation of SHC is a challenging task due to the existence of multi-phase materials i.e. both solid and liquid. The inherent problem comes from the fact of modeling the fluid filled capsules. The fluid properties for capsule cores are not considered in this paper, which is an important scope for future work.

In Abaqus software, when the inclusions are randomly distributed in RVE, the structured mesh generation is quite impossible. Moreover, when more inclusions cut the edges or boundary surfaces of RVE and opposite boundaries have different position of inclusion's cut, these lead to adopt cumbersome technique for application of periodic boundary condition.

6 Conclusion

Homogenization is a useful tool in many engineering problems. The linear homogenization tool should be carefully used keeping its limitation in mind. This is due to the fact that RVE describes constant deformation over microscopic domain.

A more realistic computational model of SHC would require extensive study of the experimental results which are being obtained through experiments in different parts of the world. Computational model of SHC can be improved by incorporating more modeling parameters known from different experiments and using various statistical tools for verifying their response on SHC.

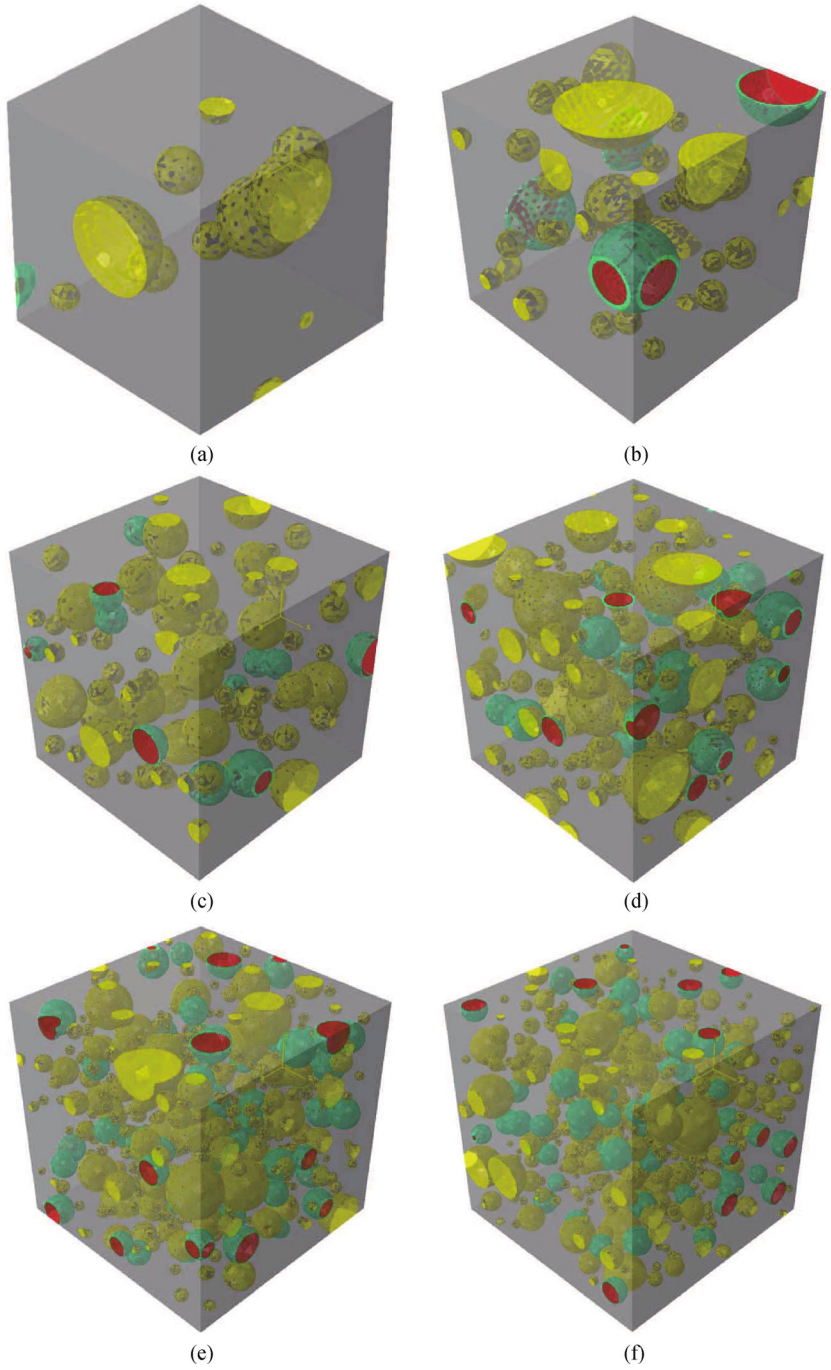

Fig. 9 3D RVEs with different RVE size. (a) "REV" size 5 mm; (b) "REV" size 8 mm; (c) "REV" size 10 mm; (d) "REV" size 15 mm; (e) "REV" size 20 mm; (f) "REV" size 25 mm (Color legend: gray = matrix, yellow = sand, green = cap. shell, red = cap.core)

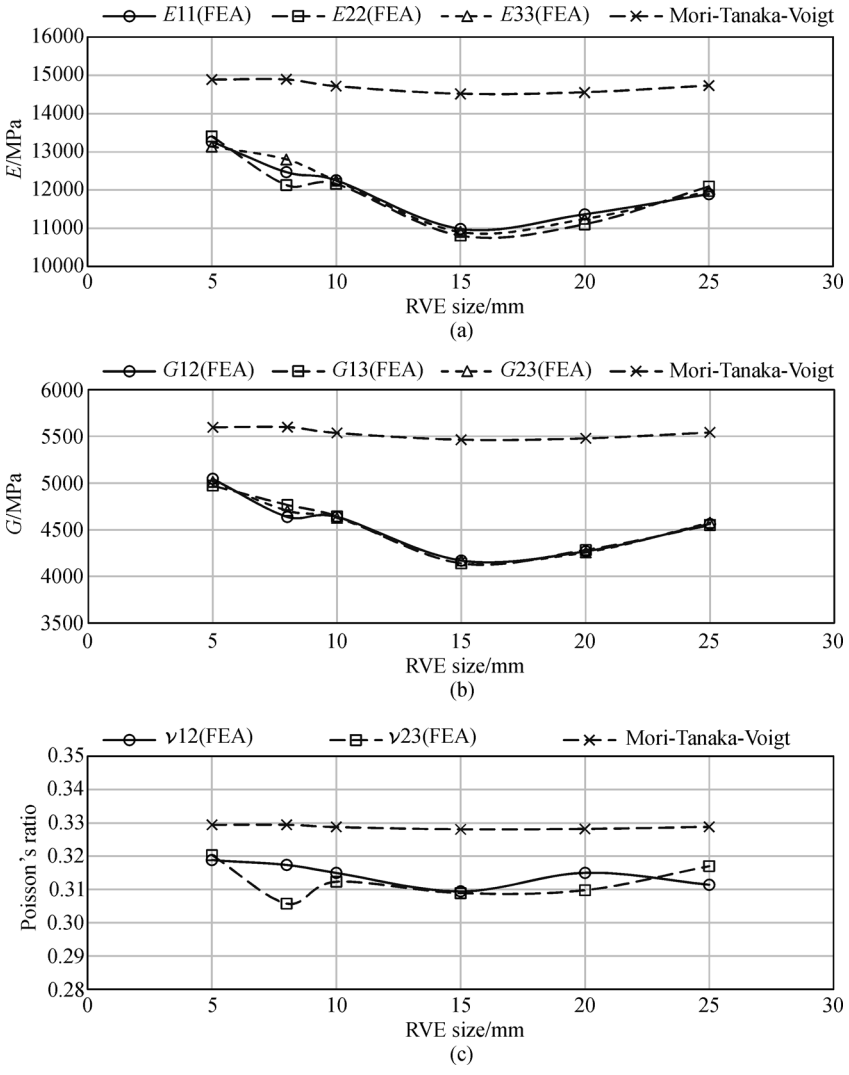

Fig. 10 The homogenized elastic properties against the RVE size obtained from FEA and analytical solution

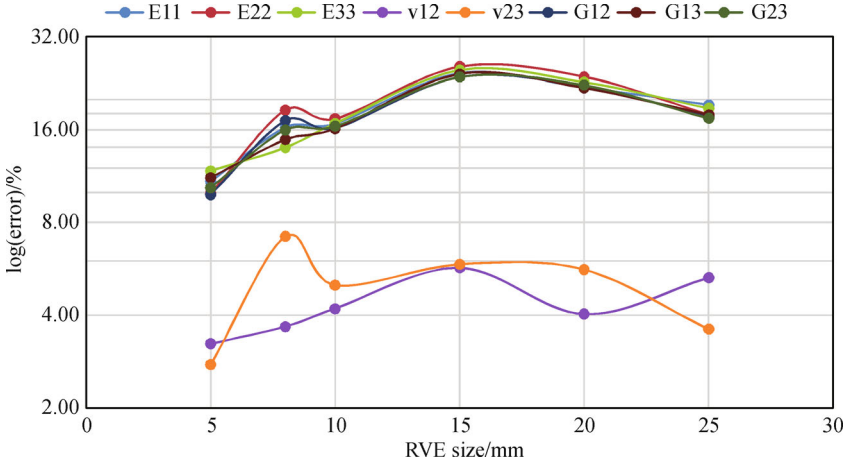

Fig. 11 Error plot of different elastic properties against RVE size

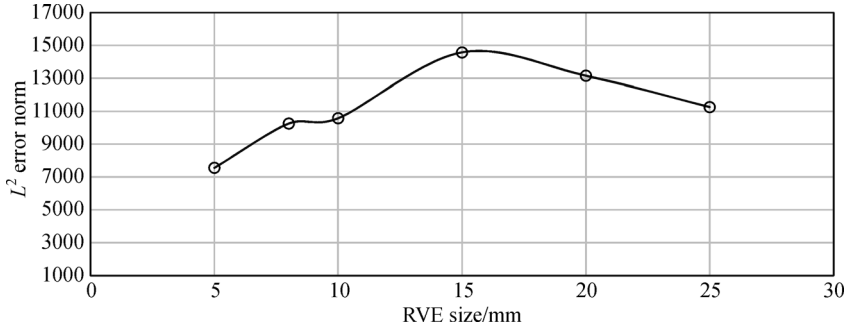

Fig. 12 L^2 error norm of elasticity tensor against RVE size

Acknowledgements The authors would like to express their gratitude to Mr. Qing Wang of Tongji University, Shanghai, China and Mr. Mohammad Silani of Bauhaus-Universität Weimar, Germany for their support. The second author would also like to acknowledge the support of the National Basic Research Program of China (Grant No. 2011CB013800).

References

1. Van Tittelboom K, De Belie N. Self-healing in cementitious materials—a review. Materials, 2013, 6(6): 2182–2217
2. Dry C. Matrix cracking repair and filling using active and passive modes for smart timed release of chemicals from fibers into cement matrices. Smart Materials and Structures, 1994, 3(2): 118
3. White S R, Sottos N R, Geubelle P H, Moore J S, Kessler M, Sriram S R, Brown E N, Viswanathan S. Autonomic healing of polymer composites. Nature, 2001, 409(6822): 794–797
4. Dry C. Procedures developed for self-repair of polymer matrix composite materials. Composite Structures, 1996, 35(3): 263–269
5. Li V C, Lim Y M, Chan Y W. Feasibility study of a passive smart self-healing cementitious composite. Composites. Part B, Engineering, 1998, 29(6): 819–827
6. Lee J Y, Buxton G A, Balazs A C. Using nanoparticles to create self-healing composites. The Journal of chemical physics, 2004, 121 (11): 5531–5540
7. Li V C, Yang E H. Self Healing in Concrete Materials. Self Healing Materials. Netherlands: Springer, 2007, 161–193
8. Gumbsch P, Pippan R, eds. Multiscale Modelling of Plasticity and Fracture by Means of Dislocation Mechanics. Springer Science & Business Media, 2011, 522
9. Suquet P M. Local and global aspects in the mathematical theory of plasticity. Plasticity today: Modelling, methods and applications, 1985, 279–310
10. Guedes J M, Kikuchi N. Preprocessing and postprocessing for materials based on the homogenization method with adaptive finite element methods. Computer Methods in Applied Mechanics and Engineering, 1990, 83(2): 143–198
11. Terada K, Kikuchi N. Nonlinear homogenization method for practical applications. ASME Applied Mechanics Division-Publications-AMD, 1995, 212: 1–16
12. Ghosh S, Lee K, Moorthy S. Multiple scale analysis of heterogeneous elastic structures using homogenization theory and Voronoi cell finite element method. International Journal of Solids and Structures, 1995, 32(1): 27–62
13. Ghosh S, Lee K, Moorthy S. Two scale analysis of heterogeneous elastic-plastic materials with asymptotic homogenization and Voronoi cell finite element model. Computer Methods in Applied Mechanics and Engineering, 1996, 132(1): 63–116
14. Kouznetsova V, Geers M G D, Brekelmans W A M. Multi-scale constitutive modelling of heterogeneous materials with a gradient-enhanced computational homogenization scheme. International Journal for Numerical Methods in Engineering, 2002, 54(8): 1235–1260
15. Yuan Z, Fish J. Toward realization of computational homogenization in practice. International Journal for Numerical Methods in Engineering, 2008, 73(3): 361–380
16. Weinan E. Principles of Multiscale Modeling. Cambridge University Press, 2011
17. THAO T D P. Quasi-Brittle Self-Healing Materials: Numerical Modelling and Applications in Civil Engineering. Dissertation for the Doctoral Degree. Singapore: National University of Singapore, 2011
18. Bakis C, ed. American Society of Composites-28th Technical Conference. DEStech Publications, Inc, 2013
19. Talebi H, Silani M, Bordas S P A, Kerfriden P, Rabczuk T. A computational library for multiscale modeling of material failure. Computational Mechanics, 2014, 53(5): 1047–1071
20. Li G. Self-healing Composites: Shape Memory Polymer Based Structures. Chichester, West Sussex, UK: John Wiley & Sons, 2014
21. Pierard O, Friebel C, Doghri I. Mean-field homogenization of multi-phase thermo-elastic composites: a general framework and its validation. Composites Science and Technology, 2004, 64(10): 1587–1603
22. Odegard G M, Clancy T C, Gates T S. Modeling of the mechanical properties of nanoparticle/polymer composites. Polymer, 2005, 46 (2): 553–562
23. Drugan, W J, Willis J R. A micromechanics-based nonlocal constitutive equation and estimates of representative volume element size for elastic composites. Journal of the Mechanics and Physics of Solids, 1996, 44(4): 497–524
24. De Bellis M L, Ciampi V, Oller S, Addessi D. First order

computational homogenization. Multi-scale techniques for masonry structures (pp. 27–74). Barcelona: International Center for Numerical Methods in Engineering, 2010

25. Hill R. Elastic properties of reinforced solids: some theoretical principles. Journal of the Mechanics and Physics of Solids, 1963, 11 (5): 357–372
26. Van der Sluis O, Schreurs P J G, Brekelmans W A M, Meijer H E H. Overall behaviour of heterogeneous elastoviscoplastic materials: Effect of microstructural modelling. Mechanics of Materials, 2000, 32(8): 449–462
27. Terada K, Hori M, Kyoya T, Kikuchi N. Simulation of the multi-scale convergence in computational homogenization approaches. International Journal of Solids and Structures, 2000, 37(16): 2285–2311
28. Huet C. Application of variational concepts to size effects in elastic heterogeneous bodies. Journal of the Mechanics and Physics of Solids, 1990, 38(6): 813–841
29. Huet C. Coupled size and boundary-condition effects in viscoelastic heterogeneous and composite bodies. Mechanics of Materials, 1999, 31(12): 787–829
30. Ostoja-Starzewski M. Random field models of heterogeneous materials. International Journal of Solids and Structures, 1998, 35 (19): 2429–2455
31. Ostoja-Starzewski M. Scale effects in materials with random distributions of needles and cracks. Mechanics of Materials, 1999, 31(12): 883–893
32. Pecullan S, Gibiansky L V, Torquato S. Scale effects on the elastic behavior of periodic and hierarchical two-dimensional composites. Journal of the Mechanics and Physics of Solids, 1999, 47(7): 1509–1542
33. Gumbsch P, Pippan R, eds. Multiscale Modelling of Plasticity and Fracture by Means of Dislocation Mechanics. Springer Science & Business Media, 2011, 522
34. Övez B, Citak B, Oztemel D, Balbas A, Peker S, Cakir S. Variation of droplet sizes during the formation of microcapsules from emulsions. Journal of Microencapsulation, 1997, 14(4): 489–499
35. Van Tittelboom K, Adesanya K, Dubruel P, Van Puyvelde P, De Belie N. Methyl methacrylate as a healing agent for self-healing cementitious materials. Smart Materials and Structures, 2011, 20 (12): 125016
36. Wang X, Xing F, Zhang M, Han N, Qian Z. Experimental study on cementitious composites embedded with organic microcapsules. Materials (Basel), 2013, 6(9): 4064–4081
37. Keller M W, Sottos N R. Mechanical properties of microcapsules used in a self-healing polymer. Experimental Mechanics, 2006, 46 (6): 725–733
38. Mindess S, Young J F, Darwin D. Response of concrete to stress. In: Concrete, 2nd ed. Upper Saddle River, NJ: Prentice Hall, 2003, 303–362
39. Powers T C, Brownyard T L. Studies of the physical properties of hardened Portland cement paste. ACI Journal Proceedings, ACI, 1947, 43(9): 845–880
40. Gilford III J. Microencapsulation of Self-healing Concrete Properties. Master's thesis, Louisiana State Univ Baton Rouge, 2012